Title
Thermal dependence of electrical characteristics of micromachined silica microchannel plates

Journal
Review of Scientific Instruments, 75(4)

ISSN
0034-6748

Authors
Tremsin, A S
Vallerga, J V
Siegmund, OHW
et al.

Publication Date
2004-04-01

Peer reviewed

Thermal dependence of electrical characteristics of micromachined silica microchannel plates

Anton S. Tremsin[a,*], John V. Vallerga[a], Oswald H. W. Siegmund[a],

Charles P. Beetz[b] and Robert W. Boerstler[b]

[a]Experimental Astrophysics Group

Space Sciences Laboratory

University of California at Berkeley, CA 94720

[b]NanoSciences Corp, 115 Hurley Road, Oxford, CT 06478

Abstract

Micromachined silica microchannel plates (MCPs) being developed by Nanosciences Corp. have a number of advantages over standard glass MCPs and open completely new possibilities in detector technologies. In this paper we present the results of our studies on the thermal properties of silica microchannel plates (sMCPs). Similar to standard glass microchanel plates the resistance of silica MCPs was measured to change exponentially with temperature with a negative thermal coefficient of -0.036 per degree Celsius,

*Electronic mail: ast@ssl.berkeley.edu

somewhat larger than that of standard glass MCPs. The resistance also decreases linearly with the applied voltage, with the voltage coefficient of -3.1×10^{-4} V^{-1}. With the knowledge of these two coefficients, our thermal model allows calculation of the maximum voltage, which can be applied to a given MCP without inducing a thermal runaway. A typical 25 mm diameter, 240 μm thick sMCP with 6 μm pores has to have the resistance larger than ~30 MΩ to operate safely at voltages up to 800 V. With this model we can also calculate the time required for a given silica MCP to reach the point of thermal equilibrium after a voltage increase. We hope that the ongoing efforts on a proper modification of the sMCP semiconducting layer will lead to the production of new MCPs with a small negative or even a positive thermal coefficient, reducing the possibility of thermal runaways of low-resistance MCPs required for high count rate applications.

I. INTRODUCTION

7

Photon counting imaging detectors with microchanel plates (MCPs) provide spatial and temporal (if required) information on each registered photon. Recent advances in the photocathode and readout technologies substantially improve the spatial resolution and extend the spectral sensitivity of the MCP detectors, making them very attractive for a number of new applications. Among those attractive features of MCP detectors are large configurable formats, photon counting, matching of curved focal planes, no cryogenics, solar blindness, and high temporal and spatial resolution. The spatial resolution of newly developed cross strip readout is currently limited only by the MCP pore size[1] (currently

on the order of 6-8 μm). The accuracy of timing can be as high as ~200 ps and the quantum efficiency is at 50% level for ultraviolet photons. New highly efficient semiconductor photocathodes, such as GaN, GaAs, GaAsP and InGaAs extend the sensitivity of MCP detectors into NUV, visible and near infrared spectral ranges.

The new emerging silicon-micromachined MCP technology developed by Nanosciences Corp. opens up completely new possibilities. The fabrication process of silica microchannel plates starts with photolithographic masking of the channel pattern on the surface of a Si wafer, well optimized by the semiconductor industry. The new micromachining process developed by NanoSciences Corp. is capable of etching high aspect ratio (length-to-diameter >100) structures in Si. The resulting MCP geometry is uniform and coherent, which leads to much better flat fields free of fixed pattern noise characteristic of glass MCPs. There is also a limit to the reduction of glass-MCP pore size (currently on the order of 6 μm), while Si micromachining can produce MCP with sub-micron pores and can produce a variety of MCP geometrical structures, for example MCPs with hexagonal 6 μm pores[2,3]. At the same time, size formats of Si microchannel plates can be substantially larger than today's standard dimensions. The etched Si MCP structure cannot be used as an electron multiplier due to excessive conductivity. After the Si MCP substrate wafer has been diced into the desired sMCP shapes, the Si matrix is completely oxidized eliminating the conducting Si in the channel walls and allowing high voltages to be supported. At the completion of the oxidation process, a CVD coating is deposited to provide the current conduction and secondary electron emitting layer.

Resulting silica MCPs can withstand high temperatures (in excess of 850 ^{o}C) required for deposition of many very promising new photocathode materials, while glass MCPs cannot be heated to temperatures higher than ~350 ^{o}C. Diamond and GaN, for example, are among those new photocathodes, which are currently being studied extensively[4,5,6] and a diamond photocathode has been already grown on a silica MCP[3]. Another attractive feature of silica microchannel plates is their low dark noise count rates. A typical MCP glass mix contains Rb and K that have radioactive isotopes generating dark noise events of ~0.2-1 event cm^{-2} s^{-1}. Si substrates are, by design, very pure and non-radioactive. Si is also a relatively low Z, low density element, so it has a low stopping power to X and gamma rays. Therefore the background rate due to the sMCP alone is much lower than that of glass MCPs.

Although silica MCPs are still in the developmental stage our earlier tests indicate that their performance is quite similar to that of standard glass microchannel pates: gain, pulse height, response and gain uniformity, and quantum detection efficiency were the same as those for glass MCPs[2,3,7,8], while sMCP background was measured to be as low as ~ 0.02 events sec^{-1} cm^{-2} without shielding[8], a significant improvement over even low noise MCP's.

In this paper we present the results of our studies on thermal properties of current sMCPs, provided by Nanosciences Corp. The microchannel plates used in this study were 40:1 L/D, 25 mm in diameter with 6 μm square pores on 8 μm centers, biased at 5-8 degrees.

II. THERMAL PROPERTIES OF SILICA MCPS: MEASUREMENTS AND CALCULATIONS

A. MCP resistance variation with temperature and voltage

The count rate capabilities of MCP detectors are known to be limited by the recharge time, which is proportional to the MCP resistance[9]. Consequently the dynamic range of MCP detectors can be extended by the reduction of the MCP resistance. However, the negative temperature coefficient of glass MCPs ultimately leads to thermal instability as the resistance is decreased. A larger amount of Joule heat is generated by low-resistance MCPs ($Q_{Joule}=(V_{MCP})^2/R$) and thermal runaway (local melting of the glass) is the result in extreme cases. At the same time accelerating bias V cannot be reduced for low-resistance MCPs since it determines the gain of microchannel plate. The knowledge of the MCP temperature coefficient allows determination of the lowest resistance at which the MCP can operate at a given accelerating bias V. The only way for the MCP to dissipate the Joule heat is through the radiative dissipation and conductive heat transfer through the contact electrodes, which are, in turn, limited to some values and cannot provide stable operation of very low resistance MCPs.

The resistance of glass MCPs was reported to depend on both temperature and applied high voltage[10,11]:

Electr. characteristics of silica MCPs

$$R_{MCP}(T_{MCP},V_{MCP}) = R_0\left[1-\alpha_v V_{MCP}\right] * \exp\{-\beta_T\left(T_{MCP}-T_0\right)\} \quad (1)$$

where R_0 is the resistance of MCP measured at V_{MCP}=0V and temperature $T_{MCP}=T_0$.

To determine the thermal coefficient, $\alpha_{V,}$ of sMCPs, we mounted them in a thermally controlled tank and measured their resistance as a function of temperature at fixed applied voltages of 100, 200 and 300V, Fig.1. The temperature of the thermostat was varied between -18 ^{o}C and +49 ^{o}C and the resistance measurements were performed after the MCPs had thermalized to the thermostat temperature. Our results indicate that the dependence of the sMCP resistance on temperature is indeed exponential. The agreement between calculated R_{MCP} from equation (1) with value of β_T = 0.036 ^{o}C^{-1} and the experimental data is quite good for all three bias voltages (Fig.1).

The experimentally measured dependence of silica MCP resistance on the applied voltage is shown by circles in Fig.2. A silica MCP with lower resistance (and thus more pronounced thermalization effect) was used in this experiment. After each voltage increment the MCPs were left to thermalize and only then the resistance was measured. Once the voltage across the MCP is increased the Joule heat generated by the MCP elevates its temperature. Increased temperature leads to the reduction of the MCP resistance, which in turn results in a larger amount of Joule heat generated, leading to a further temperature increase. The MCP resistance finally stabilizes when Joule heat is balanced by the heat dissipation through radiation and conduction:

$$Q_{Joule} = Q_{rad} + Q_{cond.} \quad (2)$$

In our experiments we used an all-plastic detector body, which effectively did not allow any heat dissipation through conduction, except for the spacer between the MCPs and the vacuum flange. Taking that into account, eq. (2) leads to the following equation:

$$\frac{V_{MCP}^2}{R_{MCP}} = 2\frac{\pi D1_{MCP}^2}{4}\sigma\varepsilon\left[T_{MCP}^4 - T_A^4\right] + \frac{K_p A_p \left(T_{MCP} - T_A\right)}{L_p} \tag{3}$$

where V_{MCP} is the voltage across microchannel plate with resistance R_{MCP}, $D1_{MCP}$ the diameter of the radiating surface (~2.0 cm in our case), T_{MCP} the temperature of the radiating MCP surface, T_A the laboratory ambient temperature (20 ^{o}C in our measurements), σ Stephan-Boltzmann constant, ε the effective thermal emittance of MCP (ε=0.4,[12]), K_p, A_p and L_p are the thermal conductivity, cross section area and thickness of the spacer (made out of peek) between the MCP and the supporting metal flange, which is assumed to be a heat sink maintained at ambient temperature T_A. The factor of 2 in the first term on the right hand side takes into account the fact that the heat is radiated from both surfaces of the MCP. Assuming the MCP is thin enough so that the temperature is uniform across its volume and substituting eq.(1) into eq.(3) we obtain:

$$V_{MCP}^2 = \left\{\frac{\pi D1_{MCP}^2}{2}\sigma\varepsilon\left(T_{MCP}^4 - T_A^4\right) + \frac{K_p A_p \left(T_{MCP} - T_A\right)}{L_p}\right\} R_0\left[1 - \alpha_v V_{MCP}\right] * \exp\left\{-\beta_T (T_{MCP} - T_0)\right\} \tag{4}$$

From equation (4) we can calculate T_{MCP} for a given voltage V_{MCP}, then find the resistance $R_{MCP}(V,T)$ from eq.(1) and compare it with experimentally measured value. Thus coefficient α_V can be found by a best fit of calculated R_{MCP} to measured data. The solid line in Fig.2 corresponds to the results of our numerical iterative calculations using eq.(1) and (4) with coefficient α_V=3.1x10^{-4} V^{-1}. There is a large discrepancy between the calculated and measured data at voltages below ~150V due to measured threshold effect at out of range low voltage operation, also observed with glass microchannel plates. The calculations predict that such an MCP will have thermal runaway at applied voltage ~1200V. In reality the thermal runaway occurs at somewhat lower voltage due to the highly localized nature of the phenomenon, while our model assumes that the temperature and resistance are completely uniform across the MCP volume and that there is no temperature gradient along MCP pores. The latter assumption is not completely true since the heat dissipation happens only on the MCP surface. Although we cannot exactly predict the voltage for thermal runaway, we still can use the described calculations for the estimation of sMCP resistance as a function of applied voltage for the biases below the thermal runaway point. For example, we can separate contributions of two terms of equation (1), shown in Fig.3: diamonds represent the dependence of the MCP resistance on the applied voltage calculated from equations (1) and (4) with α_V assumed to be equal to 0, while crosses in that graph correspond to the case when β_T is set equal to 0 (only voltage dependence of resistance is taken into account). At higher voltages the contribution of the thermal term β_T dominates over voltage term α_V and eventually leads to a runaway, while at lower voltages the contribution from the term β_T is minimal. Knowing coefficients β_T and α_V also allows us to calculate from equation (1) the MCP

resistance as a function of the MCP temperature at a fixed voltage across sMCP (Fig.4). Data of Fig.4 indicates that the resistance of silica MCP measured immediately after applying 700V bias with the initial MCP temperature of 25 and 40 degrees should result in the resistance drop by as much as 40%. If thermalization taken into account and the temperature of the MCP is measured as a function of applied voltage after the MCP has reached the thermal equilibrium the final temperature of the MCP should be calculated from both equations (1) and (4). The results of such calculations are shown in Fig.5, with the temperature of MCP plotted as a function of the applied voltage. The MCP temperature grows quasi-exponentially with the voltage increase and at ~1200V the MCP undergo a thermal runaway.

Fig.6 shows the dependence of R_{MCP} on applied voltage for different values of initial MCP resistance R_0. The same 25 mm diameter 40:1 L/D sMCP with 6 μm square pores on 8 μm period was modeled in this graph, except the initial resistance R_0 was varied. The calculation results imply that the thermal runaway for an MCP with R_0=10 MΩ will happen at voltages below 520V, while a sMCP with 60 MΩ initial resistance should be stable at voltages as high as 1000V, unless some manufacturing defects result in localized heating leading to a runaway.

B. MCP thermalization time after voltage is applied

With the knowledge of the voltage and thermal coefficients α_V and β_T we can estimate how long it takes for sMCPs to reach the thermal equilibrium after a given voltage V_{MCP}

is applied. Here again we assume that the MCP is thin so that there is no temperature gradient along the pores. Conductivity through the contact electrodes is also neglected. The temporal equation of thermal balance can be written then in the following form:

$$Q_{joule}dt = c_p^{(MCP)}\rho_{MCP}\upsilon_{MCP}dT + c_p^{(spacer)}\rho_{spacer}A_pL_p\frac{dT}{2} + \left(Q_{rad} + Q_{cond}\right)dt \tag{5}$$

where $c_p^{(MCP)}$ is the thermal capacity of sMCP, ρ_{MCP} is its density and υ_{MCP} is the volume of the MCP walls, $c_p^{(spacer)}$ is the thermal capacity of the peek spacer and ρ_{spacer} is its density. We assume that the temperature gradient across the spacer is a linear function, leading to the averaged temperature increase of the spacer to be one half of dT. Using equations (1) and (3) and integrating the equation (5) we obtain:

$$\int_0^{t_1} dt = \int_{T_0}^{T_1}\left(c_p^{(MCP)}\rho_{MCP}\upsilon_{MCP} + c_p^{(spacer)}\rho_{spacer}A_pL_p/2\right)FdT_{MCP};$$

$$F = \left[\frac{V_{MCP}^2}{R_0\left[1-\alpha_v V_{MCP}\right]*\exp\left\{-\beta_T\left(T_{MCP}-T_0\right)\right\}} - 2\frac{\pi D1_{MCP}^2}{4}\sigma\varepsilon\left(T_{MCP}^4 - T_A^4\right) - \frac{K_pA_p\left(T_{MCP}-T_A\right)}{L_p}\right]^{-1} \tag{6}$$

where T_1 is the temperature of sMCP t_1 seconds after the voltage was instantaneously increased from 0 to V_{MCP}. The value of T_1 changes in the range $[T_A,T_{max}]$, where T_{max} is the asymptotic value of the MCP temperature at the point of thermal equilibrium for a given voltage V_{MCP} (T_{max} can be found numerically from equation (4)). Equation (6) is an inverse integral equation for T_{MCP} as a function of time passed since bias is applied and can be solved numerically. For a given value of T_{MCP} from the interval $[T_A,T_{max}]$ we numerically calculate the integral on the right hand side of equation (6) and thus obtain the time required to reach the point of thermal equilibrium. The numerically calculated

temperature of a sMCP as a function of time past from the point of voltage increase T_{MCP} = T_{MCP}(t) is shown in Fig.7 for several voltages V_{MCP}.

In our calculations we used standard quartz values for heat capacity $c_p^{(MCP)}$=0.755 J g^{-1} C^{-1} and density ρ_{MCP}=2.2 g cm^{-3} (after the micromachining stage of sMCP manufacturing the entire silicon wafer is reduced to silica by thermal oxidation), the heat capacity of spacer made from peek $c_p^{(spacer)}$=1.3 J g^{-1} C^{-1} and its density ρ_{spacer}=1.31 g cm^{-3}. The volume of the walls of a square-pore MCP is found from the equation

$$\upsilon_{(MCP)} = D_{MCP} L_{MCP} \frac{w^2 + 2dw}{(d+w)^2} \tag{7}$$

where d and w are the MCP pore and wall widths, respectively, and L_{MCP} is the thickness of the plate. The MCP was assumed to have 6 μm wide square pores, 2 μm wide walls and have 80 MΩ initial resistance. Diameter of MCP was taken to be D_{MCP}=25mm and MCP thickness L_{MCP}=240 μm. The initial temperature T_A=20 ^{o}C. The results of our numerical calculations indicate that the MCP thermalization is virtually completed within 1-2 minutes for voltages below 800V, while application of higher voltages may require approximately 5-10 minutes for the MCP to reach the thermal equilibrium. The predicted thermalization time is approximately equal to what we have observed in our measurements: the MCP current was increasing during several minutes after the high voltage was applied, proving the applicability of the presented model of thermalization. However, more precise quantitative measurements of thermalization time are yet to be carried out.

III. DISCUSSION

The results of our study of thermal properties of newly developed silica MCPs indicate that these microchannel plates have negative thermal coefficient, similar to that of standard glass microchannel plates. By measuring the resistance as a function of MCP temperature for the temperatures varying between -17 and 48 ^{o}C we found that the resistance of sMCPs indeed changes exponentially with temperature - $R_{MCP}(T) \propto R_0 \exp\{-\beta_T(T_{MCP} - T_0)\}$ with the coefficient β_T=0.036 ^{o}C^{-1}. This value of thermal coefficient of sMCPs is somewhat similar to the thermal coefficient of standard glass MCPs, which was reported to be 0.02 ^{o}C^{-1} in ref. [13], 0.0175 ^{o}C^{-1} in ref. [12] and 0.0084 ^{o}C^{-1} in ref. [14]. As reported by Roth et. al.[11] the MCPs at cryogenic temperatures should have a much larger thermal coefficient, although all MCP detectors are currently operated at normal temperatures. Thus the range of temperatures at which the thermal coefficient β_T was measured for sMCPs should be sufficient for the optimisation of current detecting devices.

The coefficient α_V of sMCPs was found to be equal to 3.1x10^{-4} V^{-1}, 5 times larger than that of glass microchannel plates equal to 6x10^{-5} V^{-1} (ref. [10]). We conclude that, similar to standard glass MCPs, the stable operation of silica microchannel plates will require their resistance to be larger than ~30 MΩ for a 25 mm diameter 40:1 L/D MCP to operate safely at ~700V.

Knowing the coefficients α_V and β_T of sMCPs we can estimate with the help of described model the time required for the MCP thremalization after a given voltage was applied to MCP. The results of our calculations indicate that it takes about several minutes for the MCP to reach the point of thermal equilibrium at operating voltages.

Positive thermal coefficient would be a very attractive feature of silica MCPs since it would likely prevent local thermal runaways. Nanosciences Corp. is currently working on possible modifications of MCP pore semiconducting layer in order to produce MCPs with positive or small negative thermal coefficient. Such MCPs would be very useful for high counting rate applications since their resistance can be reduced to very small values (for which existing glass MCPs become thermally unstable) leading to a substantial reduction of the recharge time and increasing the local counting rate capabilities.

ACKNOWLEDGMENTS

This work was supported by NASA grant NAG5-9149 and NAG5-12710.

REFERENCES

1. O. H. W. Siegmund, A. S. Tremsin, J. V. Vallerga, R. Abiad and J. Hull, Nucl. Instr. and Meth. **A 504**, 177 (2003).

2. C. P. Beetz, R. Boerstler, J. Steinbeck, B. Lemieux, D. R. Winn, Nucl. Instr. and Meth. **A 442,** 443 (2000).
3. A. S. Tremsin, J. V. Vallerga, O. H. W. Siegmund, C. P. Beetz, R. W. Boerstler, Proc. SPIE **4854,** 215 (2002).
4. A. S. Tremsin, O. H. W. Siegmund, Proc. SPIE **4139**, 16 (2000).
5. M. P. Ulmer, B. W. Wessels, B. Han, J. Gregie, A. S. Tremsin and O. H. W. Siegmund, Proc. SPIE **5164,** "UV/EUV and Visible Space Instrumentation for Astronomy II", San Diego, August 2003.
6. O. H. W. Siegmund, A. S. Tremsin, A. Martin, J. Malloy, Proc. SPIE **5164,** "UV/EUV and Visible Space Instrumentation for Astronomy II", San Diego, August 2003.
7. A. W. Smith, C. P. Beetz, R. W. Boerstler, D. R. Winn, J. W. Steinbeck, Proc. SPIE **4128,** 14 (2000).
8. O. H. W. Siegmund, A. S. Tremsin, J. V. Vallerga, C. P. Beetz, et. al., Proc. SPIE **4497,** 139 (2002).
9. A. S. Tremsin, J. F. Pearson, G. W. Fraser, W. B. Feller, P. White, Nucl. Instr. And Meth. **A 379,** 139 (1996).
10. A. Sardella, M. Bassan, L. Giudicotti, L. Lotto, R. Pasqualotto, Proc. SPIE **2551,** 273 (1995).
11. P. Roth, G. W. Fraser, Nucl. Instr. and Meth. **A 439,** 134 (2000).
12. J. F. Pearson, G. W. Fraser, M J. Whiteley, Nucl. Instr. and Meth. **A 258,** 270 (1987).
13. O. H. W. Siegmund, Proc. SPIE **1072,** 111 (1989).
14. D. C. Slater, J. G. Timothy, Rev. Sci. Instr. **64,** 430 (1993).

Figure Captions

Fig.1. The resistance of silica MCP measured as a function of MCP temperature at three different voltages. The lines correspond to the equation shown in the graph with the same exponential coefficient of β_T=0.036 $^oC^{-1}$.

Fig.2. The resistance of an 80 MΩ, 40:1 L/D 25 mm diameter silica MCP with 6 μm pores measured (circles) and calculated (solid line) as a function of MCP bias V_{MCP}. The measurements of R_{MCP} were performed after the MCP (mounted in a chevron stack) reached the thermal equilibrium at a given voltage V_{MCP}. Thermal coefficient β_T=0.036 $^oC^{-1}$ and voltage coefficient α_V=3.1x10^{-4} V^{-1} are used in the calculations of $R(V_{MCP})$ from equations (1) and (4). The predicted thermal runaway voltage of 1250V is the upper limit. The runaway will likely to happen at lower voltages due to the presence of temperature gradient and local heating not taken into account in calculations.

Fig.3. Calculated resistance of the same as in Fig.2 silica MCP as a function of MCP bias V_{MCP}. Thick line - contributions from both terms α_V and β_T are taken into account; Crosses - contribution from only the voltage term α_V (β_T is set to 0); Diamonds - contributions from only temperature term β_T (α_V is set to 0).

Fig.4. Calculated resistance of the same as in Fig.2 silica MCP measured immediately after a voltage of 700V is applied across it, as a function of initial MCP temperature.

Fig.5. Calculated temperature of the same as in Fig.2 silica MCP at the point of thermal equilibrium as a function of applied bias. The Joule heat generated by MCP is dissipated by radiation from the MCP surface and conduction through the mounting structure. The ambient temperature T_A is taken to be 20 ^{o}C. The MCP thermal runaway is predicted to occur below ~1250V.

Fig.6. Calculated resistance of a 40:1 L/D 25 mm diameter silica MCP with 6 μm pores (mounted in a chevron stack) as a function of MCP bias V_{MCP} for different values of initial resistance R_0. The initial resistance determines the maximum voltage, which can be applied to the MCP without inducing a thermal runaway.

Fig.7. Calculated temperature of the same as in Fig.2 silica MCP as a function of time after V_{MCP} is increased from 0 to a given voltage, indicated on the graph. For voltages below ~800 V the MCP reaches the thermal equilibrium in a few minutes.

Fig.1

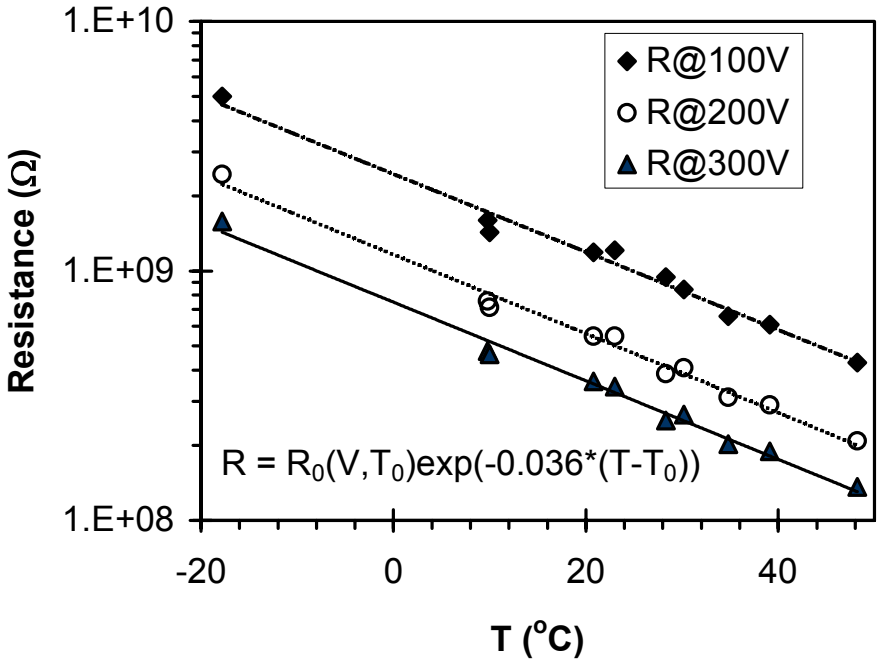
1.E+10
1.E+09
1.E+08
Resistance (Ω)
R@100V
R@200V
R@300V
R = R0(V,T0)exp(-0.036*(T-T0))
-20
0
20
40
T (°C)

Fig.2

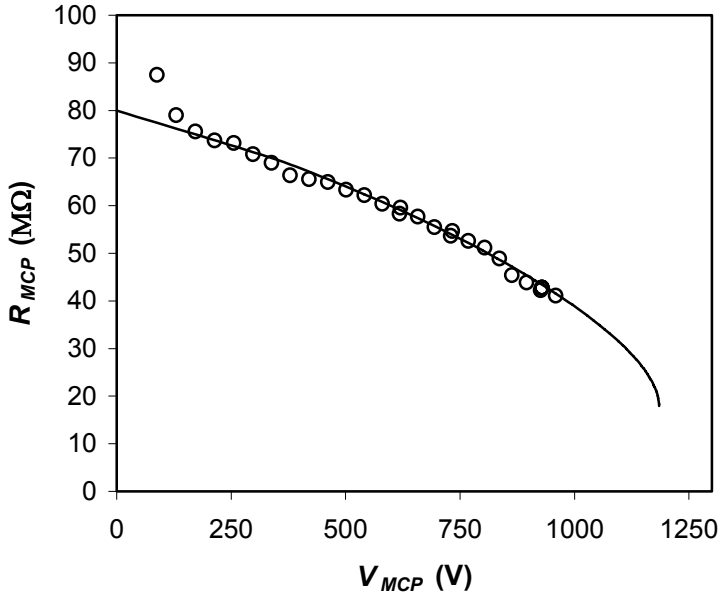
100
90
80
70
60
50
40
30
20
10
0
0
250
500
750
1000
1250
R_{MCP} (MΩ)
V_{MCP} (V)

Fig.3

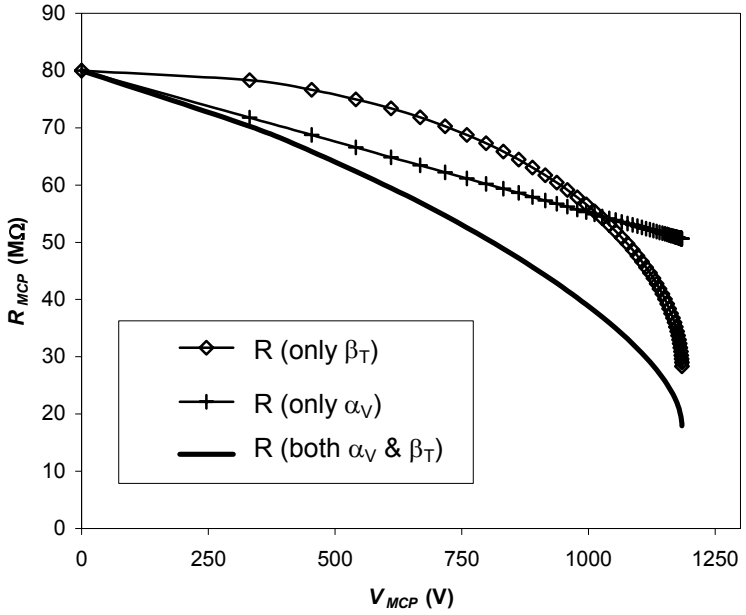
90
80
70
60
50
40
30
20
10
0
0
250
500
750
1000
1250
R_{MCP} (MΩ)
V_{MCP} (V)
R (only β_T)
R (only α_V)
R (both α_V & β_T)

Fig.4

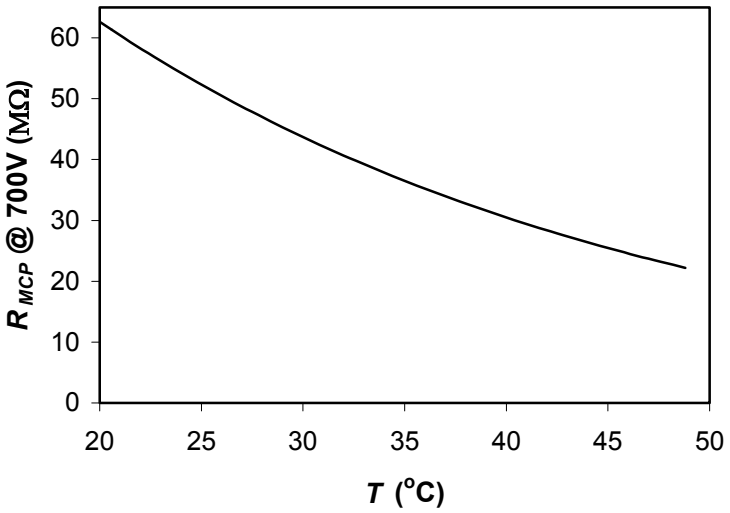

Fig.5

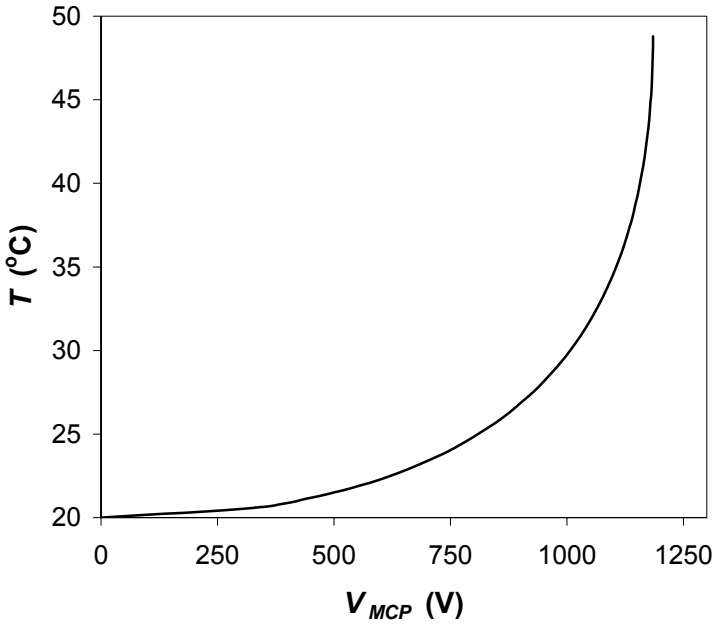

Fig.6

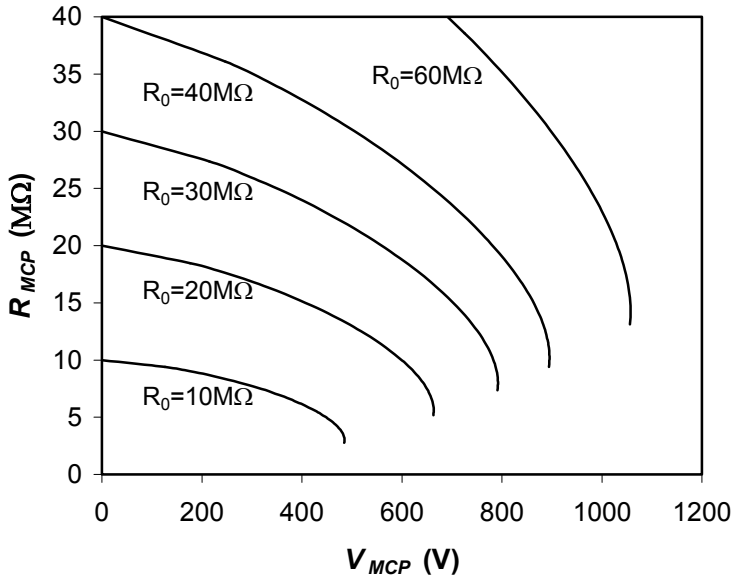
40
35
30
25
20
15
10
5
0
0
200
400
600
800
1000
1200
R0=60MΩ
R0=40MΩ
R0=30MΩ
R0=20MΩ
R0=10MΩ
R MCP (MΩ)
V MCP (V)

Fig.7

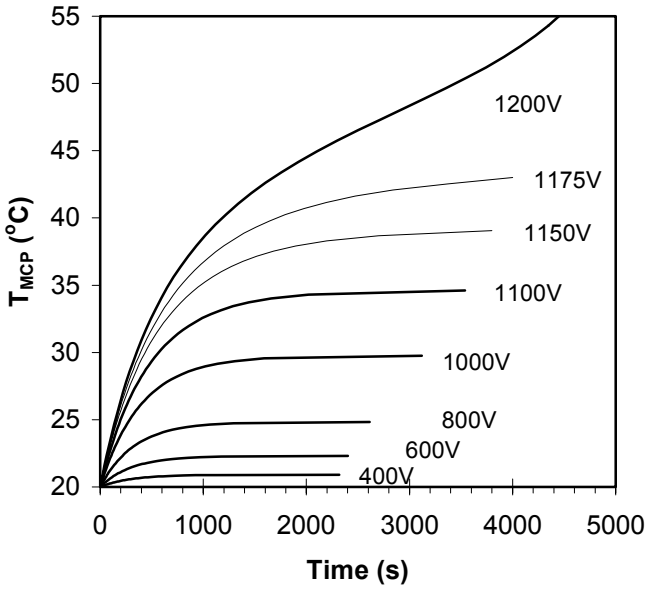
55
50
45
40
35
30
25
20
T_{MCP} (°C)
0
1000
2000
3000
4000
5000
Time (s)
1200V
1175V
1150V
1100V
1000V
800V
600V
400V